J. Membrane Biol. 40, 97–116 (1978)

Ionic Selectivity, Saturation, and Block in Gramicidin A Channels

II. Saturation Behavior of Single Channel Conductances and Evidence for the Existence of Multiple Binding Sites in the Channel

Erwin Neher*, John Sandblom, and George Eisenman

Abteilung Molekularer Systemaufbau, Max-Planck-Institut für Biophysikalische Chemie, Göttingen, Germany, Department of Physiology and Medical Biophysics, University of Uppsala, Sweden, and Department of Physiology, UCLA Medical School, Los Angeles, California

Received 22 August 1977

Summary. A theory, recently developed by Sandblom, Eisenman and Neher (1977) for the conductance of single gramicidin A channels predicts three limiting behaviors of the relation between conductance and salt concentration. These are: (i) a saturating behavior resembling a simple adsorption isotherm at medium and high concentrations, (ii) a decrease in conductance at the highest obtainable concentrations and (iii) deviations from the isotherm at very low concentrations. Features i and ii have been described before. Experimental evidence for point iii is given here. The new feature points towards interactions among ions in the channel at ionic concentrations as low as 1–10 mM.

Particular emphasis is given to the behavior at very low salt concentrations and the experimental problems encountered in this situation. In addition, mutual blocking effects among monovalent ions in symmetrical salt mixtures are characterized and found to be in satisfactory agreement with theoretical expectations, based upon the single salt conductance data presented here and zero-current potentials in salt mixtures to be described in a subsequent paper.

The conductance of single gramicidin A channels, and its dependence on the concentration of monovalent salt solutions has been characterized by Hladky and Haydon (1972). The principal finding of this investigation was a saturating behavior of the conductance *vs.* concentration curve and, for some salts, even a decrease of conductance at very high concentrations. Those two features were explained by a theory, developed by Hladky (1972), which assumes two binding sites for monovalent ions inside the channel.

* *Address for reprint requests:* Max-Planck-Institut für Biophysikalische Chemie, 34, Göttingen, Germany.

0022-2631/78/0040-0097 $4.00

The theory could not explain concentration-dependent permeability ratios which were observed by Myers and Haydon 1972. In addition, another complicated phenomenon, the mutual blocking of ions within the channel, was described by Neher (1975) and Andersen (1975). These manifestations of ionic interaction have recently aroused special interest since the very same phenomena, which are *saturation, concentration dependent permeability ratios*, and *block*, have been observed in squid axon (Hille, 1975, Cahalan & Begenesich, 1976). A model, developed for the gramicidin channel by Sandblom, Eisenman and Neher (1977), accounts for the three features mentioned above.

In the present communication experimental data on single channel conductance in symmetrical salt solution will be presented and interpreted in terms of the theory of Sandblom *et al.* (1977). A companion paper (Eisenman, Sandblom & Neher, *to be published*) will present data on potential measurements in salt gradients and compare the results from both classes of experiment. The physical implications of the quantities measured (rate constants, binding constants, energies of interaction) will be discussed in the companion paper.

Preliminary reports of some of the results have appeared (Eisenman, Sandblom & Neher, 1976; Eisenman, Sandblom & Neher, 1977).

Materials and Methods

Methods

Black lipid membranes were formed from solutions of 14 mg/ml glycerylmonooleate in hexadecane with standard techniques. The requirement of measuring single channel conductance (<5 pS) in very dilute solution made it necessary to alter some aspects of the usual chamber configuration, which will be described in some more detail.

Prerequisites for low noise measurements are (i) a small membrane area and (ii) small capacitance between one of the chambers – together with the electric leads connecting it with the amplifier input – and ground (*see also* Fettiplace *et al.*, 1975). In order to meet these requirements, a concentric arrangement of a larger outer chamber and a small cylindrical inner chamber was used. The small inner chamber was hooked directly onto the input jack of an amplifier headstage which in turn was mounted onto a micromanipulator (*see* Fig. 1). The inner chamber, which also contained a 0.2 mm diam. hole for membrane formation was fabricated from polypropylene disposable syringes as described in the legend to Fig. 1. The concentric arrangement has the advantage that the outer chamber, which is connected to a low impedance voltage source, serves as a shield to the inner chamber.

After formation of the membrane, a voltage of 50 mV was applied and gramicidin was added to the outer chamber (volume 18 ml) from ethanolic stock solution (10–40 ng/ml). The stock solution was added in aliquots of 20 µl, until discrete current steps

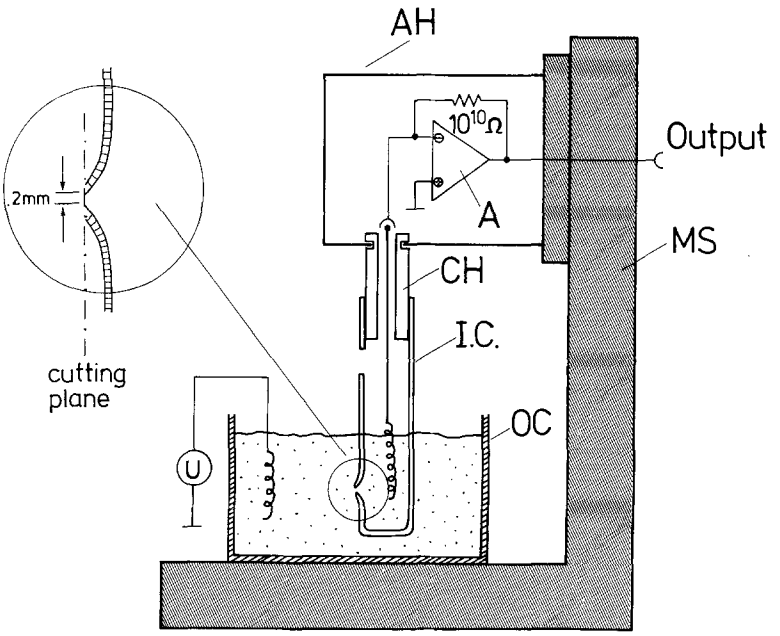

Fig. 1. Schematic diagram of the experimental arrangement with cylindrical inner chamber (*IC*), outer chamber (*OC*), micromanipulator stand (*MS*), amplifier headstage (*AH*) and chamber holder (*CH*). The chamber holder is a Teflon insulated connector to the amplifier input, onto which the inner chamber can be pushed. The inner chamber is fabricated from the cylinder of a 5-ml disposable syringe (polypropylene) into which a very small hole with extremely sharp, uniform edges can be made. The method of hole formation is indicated in the insert: The wall of the syringe is bulged with a suitable glass tool after slight heating. Subsequently, the protrusion is cut with a razor blade, repetitively removing slices, until an opening appears. The resulting geometry secures a very stable and symmetric meniscus, the size of which can be controlled by slight adjustments of hydrostatic pressure (moving the chamber up and down with the micromanipulator). This way, membranes of 20–100 μm diameter can be made reproducibly. The amplifier is a Burr Brown Model 3523L or an Analog Devices Model 515 microcircuit. Peak-to-peak background noise (including endogeneous membrane noise) smaller 0.01 pA at 8-Hz bandwidth can be obtained with this arrangement (*see* insert, Fig. 2)

due to opening and closing of individual gramicidin channels occurred. Depending on electrolyte concentration, a total volume of 20 to 180 μl had to be added such that ethanol concentration in the chamber stayed below 1%. The most frequent value of current step sizes was measured for +50 and −50 mV. Conductance was calculated from these two values, except where stated otherwise. This measurement was repeated several times for at least 2 different membranes (in more than 90% of the measurements), and a mean value was calculated. For a change of solution both chambers were emptied, cleaned, and refilled. Cleaning consisted of successive rinses in water, methanol, chloroform/methanol 2:1, and hexane, and subsequent drying in a jet of filtered nitrogen. Measurements were taken at room temperature (22–26 °C). If room temperature deviated from 23 °C by more than 0.5 °C, values were standardized to 23 °C, assuming a Q_{10} of 1.36 (Hladky & Haydon, 1972).

Materials

The lipid used was glycerylmonooleate (GMO) from Sigma and, in a control experiment, GMO synthesized by H.J. Eibl, Göttingen. Both lipids were pure as indicated by thin layer chromatography. Hexadecane was obtained from Merck as reference substance for gas chromatography. The hexane used for cleaning was a "Baker Analyzed Reagent." Valine gramicidin A was a sample kindly provided by E. Gross, NIH. Ethanol was analytical grade from Merck used either directly or after redistillation (*see below*). Water was triply distilled (twice from alkaline and acid $KMNO_4$, respectively) in most experiments. Control experiments with water from a Millipore water system gave comparable results. Salts from a variety of sources and with different purities were used: LiCl and $LiNO_3$ from MA[1], NaCl from MA, NaAc (sodiumacetate) from MS, KCl from MS and BA, KF from MS and MAR, KNO_3 from MS, KAc from BA and RH, RbCl from MA and PRM, CsCl from MS, TlCl from MA and VAU, TlF from ICN-K & K (ultrapure), $TlNO_3$ from VAU, and $TlClO_4$ from ICN-K & K (purity not specified).

Precautions at Low Ionic Strength

Conductance values at low salt concentrations (1–10 mM) had a tendency to increase slowly with the age of the membrane over a time range of 10–30 min. This time dependent process could be reset by reformation of the membrane with new lipid or by wiping the membrane and the support with an air bubble (which necessarily led to interference colors and reformation of a membrane). A possible explanation for this effect is that surface active, negatively charged impurities adsorbed to the membrane, either from the hydrocarbon or from the aqueous phase. Thereby cation concentrations would be increased in the immediate neighborhood of the membrane. Attempts to determine the origin of the postulated contamination failed. These attempts consisted of using different sources of distilled water, different sources of chromatographically checked lipid, purifying hexadecane on an aluminiumoxide column, roasting the salt, and using a Teflon chamber instead of the polypropylene cell. It was noticed, however, that the time-dependent effects were much smaller and developed more slowly when as little lipid solution as possible was applied during membrane formation. Also, the situation improved when using redistilled ethanol for the gramicidin stock solution. Therefore, lipid was applied by means of a microliter syringe during experiments at low ionic strength. An effort was made to take measurements as soon as possible after membrane formation, in a time span during which conductance values had not changed by more than 5%. This procedure is contrary to common practice, which tends to wait for a steady state to develop. It seems justified here, however, due to indications that the time-dependent changes are artifactual. Differences between some numerical values reported here and in the preliminary publications are due to the fact that previous measurements were obtained in the usual way, i.e., with aged membranes.

---

1 Abbreviations: MA (Merck analytical grade), MS (Merck suprapure), ML (Merck lab grade), BA (Baker analyzed), RH (Riedel de Haen, analytical grade), MAR (Mallinckrodt analytical reagent), ICN-K & K (K & K Laboratories), VAU (Ventron-Alfa, ultrapure), PRM (Penn Rare Metals, ultrapure).

Results

Channel Conductance as a Function of Ionic Activity when a Single Salt is Present Symmetrically on Both Sides of the Membrane

The theory developed by Sandblom *et al.* (1977) predicts three limiting behaviors in the high, medium, and low concentration ranges, respectively. A decreased conductance for the highest concentrations and a saturating relationship (like a simple binding curve) at medium con-

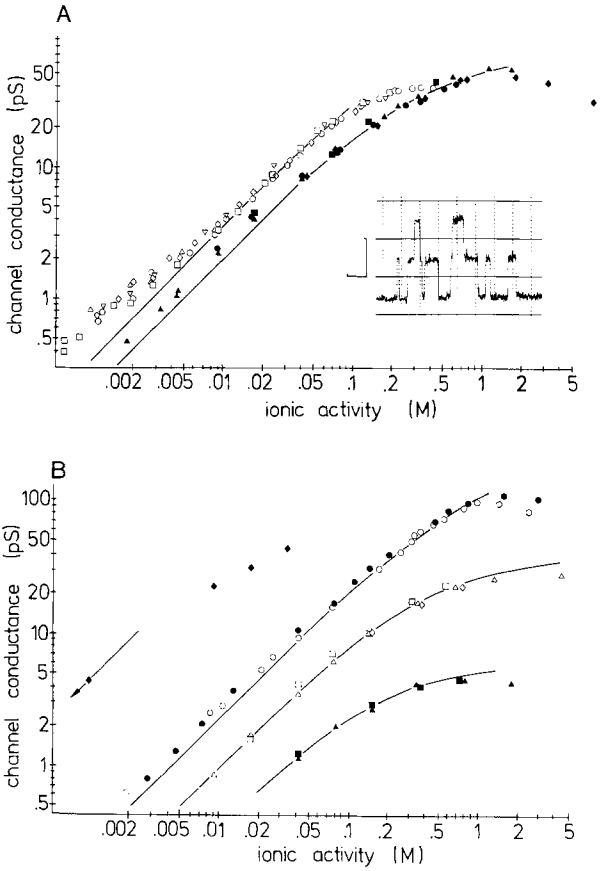

Fig. 2. Double logarithmic plot of single channel conductance *vs.* salt ionic activity. (*A*): Plot of Tl^+-salts (open symbols): $-\triangle-$, TlCl; $-\circ-$, TlF; $-\square-$, $TlNO_3$; $-\diamond-$, TlAc; and $-\triangledown-$, $TlClO_4$) and K^+ salts (solid symbols) $-\blacktriangle-$, KCl; $-\bullet-$, KF; $-\blacksquare-$ KNO_3 and $-\blacklozenge-$, KAc). For the pooled data of each cation species a single site binding curve is drawn (continuous line) which approximates the data best in the medium concentration range (50 mM – 1 M). *Insert:* Recording in 1.6 mM TlAc at 50 mV membrane potential for demonstration of the reliability of low concentration data. Calibrations: 50 fA ($5 \cdot 10^{-14}$ A) and 5 sec. (*B*): Same for HNO_3 $-\blacklozenge-$, CsCl $-\circ-$, RbCl $-\bullet-$, NaCl $-\triangle-$, $NaNO_3$ $-\square-$, NaAc $-\diamond-$, LiCl $-\blacktriangle-$, and $LiNO_3$ $-\blacksquare-$. Note the deviations at low concentration for Tl^+ salts, CsCl and K^+ salts

Table 1. Single channel conductance (pS) in symmetrical

Salt							
Conc. [mM]	HNO_3	LiCl	$LiNO_3$	NaCl	$NaNO_3$	KCl	KF
1	4.4±0.2						
2						0.48±0.02	
3						0.72±0.02	
5						1.14±0.03	
10	22.3±0.2			0.84±0.02		2.15±0.02	2.38 ±0.03
15							
20	31 ±0.2			1.63	1.6 ±0.1	4.01±0.05	4.24 ±0.06
30							
50		1.11±0.02	1.24±0.1	3.44±0.04	4.04±0.1	8.03±0.03	8.54±0.25
100		1.93±0.03		6.11±0.05	7.0 ±0.05	12.3 ±0.2	13.1 ±0.3
200		2.60±0.02	2.96±0.01	10.24±0.05	11.0 ±0.2		20.6 ±0.2
500		4.10±0.05	4.05±0.08	17.20±0.05	17.6 ±0.3	33.15±0.4	30.7 ±0.3
1000		4.47±0.02	4.48±0.15	22.70±0.4	23.1 ±0.3	45.9 ±0.5	40.7 ±0.2
2000		4.42±0.02		25.80±0.3		52.2 ±0.3	
3000						51.9 ±0.4	
5000				27.4			

centrations has been described for 1.1-electrolytes in previous work (Hladky & Haydon, 1972; Hladky, 1972; Läuger, 1973). The new feature, demanded by the theory, is a deviation from the binding curve towards higher conductance values for very low concentrations. These deviations are a consequence of additional binding sites in the model. They have so far been overlooked, since experiments were not extended to low enough ionic concentrations. Fig. 2*A* shows a double logarithmic plot of conductance *vs.* ionic activity for the Tl^+-salts (open symbols) TlCl, TlF, $TlNO_3$, TlAc and $TlClO_4$ and for the K^+-salts (closed symbols), KCl, KF, KNO_3 and KAc. (For a discussion of the activity corrections used, *see* the Appendix). Best fits of simple binding curves (1-site) to the medium concentration range for the pooled Tl^+ and K^+-data are given as continuous lines in each case. It is evident that Tl^+-data deviate strongly, and that K^+-data deviate somewhat, from the binding curve at low concentrations. Data for nitric acid and cesium-, rubidium-, sodium-, and lithium-salts are given separately for better presentation in Fig. 1*B*. Here both cesium and rubidium salts show systematic deviations from ideal behavior at low concentration, whereas no such deviations can be observed for Li^+- and Na^+-salts in the accessible concentration range.

single salt solutions, 23 °C; mean ±SE of mean[a]

KAc	RbCl	CsCl	TlCl	TlF	$TlNO_3$	TlAc	$TlClO_4$
			0.82±0.04	0.64±0.04	0.53±0.02	0.67±0.04	0.73
		0.62±0.04	1.28±0.11	0.94±0.02	0.92±0.02	1.27±0.03	1.08±0.02
	0.78±0.02		1.36±0.05	1.48±0.15	1.27±0.02	1.39±0.09	1.42±0.02
	1.26±0.04		2.16±0.05	1.8 ±0.02	1.86±0.05	2.05±0.02	
	2.52±0.03	2.42±0.06	3.58±0.11	3.2 ±0.2	3.23±0.06	3.59±0.13	3.79±0.01
	3.67±0.02				4.53±0.04	5.05±0.15	
				5.64±0.03		6.32±0.4	7.72±0.1
	6.7 ±0.05			8.02±0.03	8.6 ±0.04	8.44±0.25	10.3 ±0.4
8.07±0.08	10.6 ±0.2	9.3		12.0 ±0.1	13.62±0.05	13.1 ±0.9	
13.2 ±0.3	17.6 ±0.4	15.8 ±0.1		19.8 ±1	21.8	21.5 ±0.2	23.9 ±0.7
20 ±1.5	30.1 ±0.4			29.1 ±0.3	29.4 ±0.5		30 ±0.2
32.0 ±0.3	54.5 ±0.2	48 ±1		37.1 ±0.3			
43.0 ±0.4	81.3 ±1.4	72.3 ±0.7		38.4 ±0.1			
46.1 ±1		95.6 ±0.3					
40.8 ±0.5	107.3 ±0.2	94 ±0.5					
29.5 ±0.3	101 ±1	81.8 ±0.4					

[a] Not all data displayed in Figs. 2 and 3 are represented here, since this table had to be limited to standardized concentration values. In some cases, when data were available at concentrations sufficiently close (deviations <20%) to the standard ones, conductance values were corrected for the difference, and adopted into the table.

Representative conductance values for some of the salts studied are given in Table 1.

Membrane conductance in symmetrical salts of group Ia cations and H^+: In order to evaluate the parameters of a curve with multiple binding, a representation of conductance *vs.* conductance divided by ionic activity, analogous to the Eadie-Hofstee-type of kinetic representation (Zeffren & Hall, 1973, p. 67) is appropriate. Figure 3 shows four examples for such plots. For two salts, NaCl and LiCl (Fig. 3*A*), no deviations from a simple binding curve are apparent in the medium and low range. The Eadie-Hofstee representation is a straight line. In the other cases (CsCl, RbCl, in Fig. 3*C*; K^+-salts in Fig. 3*B*, and Tl^+-salts in Fig. 3*C*) the relation is clearly nonlinear. The continuous lines in Fig. 3*B–D* are fits of Eq. (36) from Sandblom *et al.* (1977),

$$G = \frac{P_1 a_x + P_2 a_x^2 + P_3 a_x^3}{1 + 2K_1 a_x + K_2 a_x^2 + 2K_3 a_x^3 + K_x a_x^4} \tag{1}$$

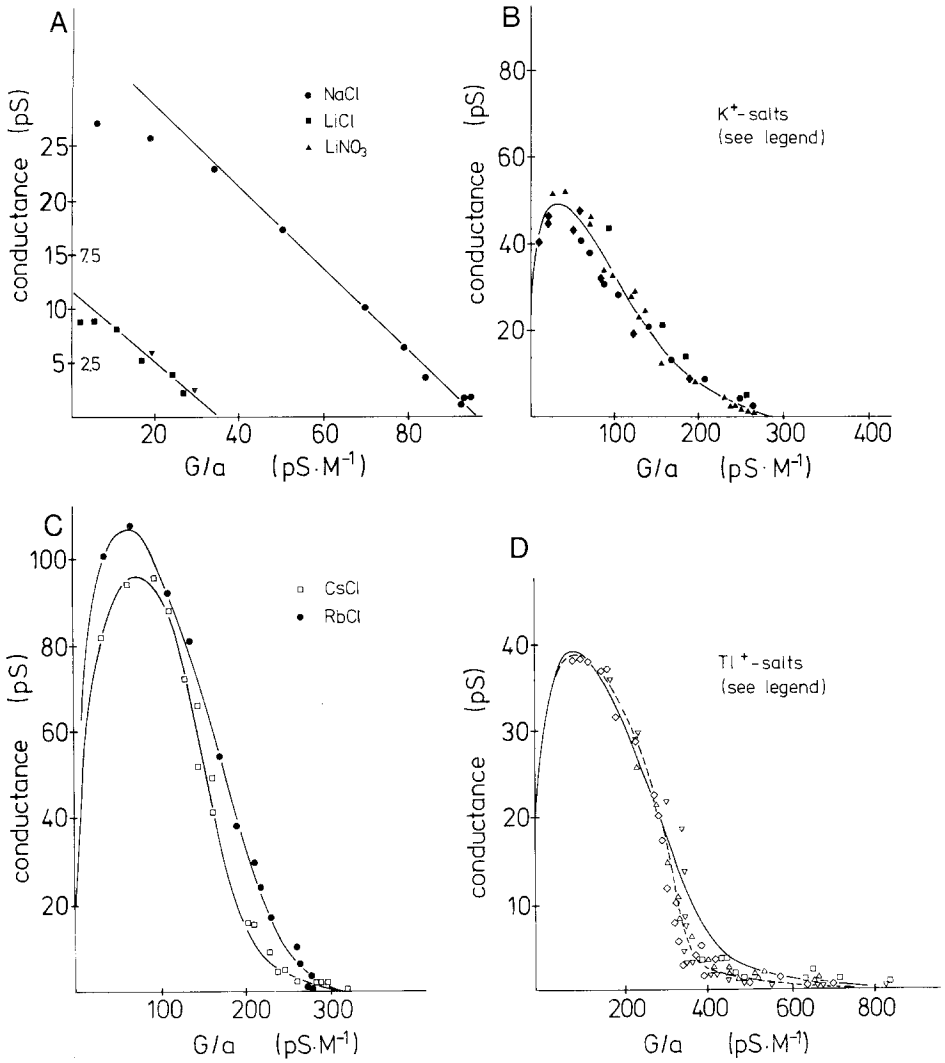

Fig. 3. Eadie-Hofstee representation [conductance *vs.* conductance/ionic activity (G/a)] for some of the data. A simple binding curve results in a straight line in this plot, with the y intercept indicating the maximum obtainable conductance, and the negative slope giving the dissociation constant. This representation is particularly useful in the present context, since the x coordinate (G/a) is proportional to the permeability of the ion under study. Theoretical curves (solid) are either straight lines (*A*) or fits according to Eq. (1), (*B*, *C*, *D*) with parameters as given in Table 2. (*A*): Plots of NaCl, LiCl, and $LiNO_3$ data. Numbers on the left side of the y axis apply to Na^+, those on the right side to Li^+. (*B*): Pooled K^+ data (−▲−, KCl; −●−, KF; −■−, KNO_3; −◆−, KAc). (*C*): Same for CsCl and RbCl data. (*D*): Pooled Tl^+ data (−□−, TlCl; −◇−, TlF; −▽−, $TlNO_3$; −△−, TlAc). The solid line is the best fit within the theory of Sandblom *et al.*, 1977 (parameters from Table 2). The broken line is a fit of the extended theory, allowing for anion binding. Parameters (Eisenman *et al.*, 1978): $G^0 = 0.8$ pS; $K^0 = 1100\ \text{M}^{-1}$; $G^h = 54$ pS; $K^h = 5.5\ \text{M}^{-1}$; $K^\infty = 0.58\ \text{M}^{-1}$; anion binding constant $K_a = 5\ \text{M}^{-1}$

to the data points. The parameters of Eq. (1) are not all independent from one another (*see* Sandblom *et al.*, 1977). However, there are five independent parameters which have an intuitive physical meaning and can be extracted from Eadie-Hofstee plots. They are therefore used for fitting: a binding constant K_x and a limiting conductance G_x at both the low (K_x^0, G_x^0) and the high (K_x^h, G_x^h) concentration end, and an additional binding constant K_x^∞ which causes a decrease of conductance as concentration is increased to highest values. The parameters of Eq. (1) are related to the parameters used for the fit through the relations (*see* Sandblom *et al.* (1977), Eqs. (42), (44), (46) and the footnote on page 405 of that publication):

$$P_1 = G_x^0 \qquad K_1 = K_x^0/2$$
$$P_2 = \sqrt{P_1 P_3} \qquad K_2 = K_1^2$$
$$P_3 = 2K_3 G_x^h \qquad K_3 = K_1^2 \cdot K_x^h/2$$
$$K_4 = 2K_3 K_x^\infty.$$

Numerical values for binding constants and limiting conductances in both the high and low concentration regions for the different cations (different anions pooled) are given in Table 2. In those cases, where the data could be fitted by a single binding curve (Li^+- and Na^+-salts) the constants were interpreted as K^h or G^h, respectively. This is somewhat arbitrary, since K^0 and K^h converge (*see* Table 2, *compare* Fig. 11 of Eisenman, Sandblom & Neher, 1978) when considering the series Cs^+, Rb^+, K^+ – which makes the distinction between high and low binding constant irrelevant for Na^+ and Li^+.

The theory of paper I of this series (Sandblom *et al.*, 1977) can be seen to be entirely satisfactory to describe all the data of the group *Ia* cation salts.

Table 2. Parameters used for fitting conductance data in symmetrical single salt solutions

	G^0 (pS)	K^0 (M^{-1})	G^h (pS)	K^h (M^{-1})	K^∞ (M^{-1})
Li^+ [a]			5.9	5.9	
Na^+ [a b]			36	2.9	≈0.3
K^+	6.8	40.4	84.7	1.48	0.27
Rb^+	5.3	57.3	228	0.91	0.33
Cs^+	3.33	100	230	0.83	0.32
Tl^+ [a]	0.8	1100	77	5.1	1.2

[a] Pooled data from differing anions.

[b] Note that values for Na^+-acetate given in a previous publication (Neher, 1975) are off by a factor of two due to an error in solution concentrations (*erratum in press* in *Biochim. Biophys. Acta*).

Membrane conductance in symmetrical Tl^+-salts: Deviations from simple behavior as shown in the last section, show up most strongly for Tl^+-ions. Figure 3*D* gives an Eadie-Hofstee representation of our Tl^+ data, pooling different anions. The superimposed theoretical curve (solid) shows that the data can be reasonably fitted by a theoretical curve according to Eq. (1). However, there are systematic deviations particularly in the region of transition between low and medium concentration ranges.

When considering single salts (different anions) individually, systematic trends are observed in Figure 3*D*. Fluoride points are on the left and lower end, whereas nitrate points are consistently on the higher side. A possible explanation for this trend is an influence of the anion on the properties of the postulated cationic binding site (Eisenman, *et al.*, 1978). An extension to the theory has been worked out which allows for anion binding at the channel entrance, when the outer binding site is occupied by a cation (Sandblom & Eisenman, *unpublished*). Qualitatively, the binding of an anion would stabilize cations bound to the channel, increasing cationic binding constants (in the multiply loaded channel states). This would lead to an increased conductance at intermediate concentrations. A fit of the extended theory to the fluoride data is included in Fig. 3*D*. It assumes an anion binding constant K_a of $5\,\text{M}^{-1}$. It further assumes both K^h_{Tl} and the peak of the central barrier to be lowered by a factor of two in the anion-bound state. Values for the other constants used in this fit are indicated in the figure legend.

The Limiting Behavior at Low Concentrations is Not an Artifact

Very low salt concentrations (5–10 mM) are required to reveal the characteristic deviations from simple behavior, as presented in the last two sections. Caution is therefore warranted, since under those conditions a number of otherwise negligible influences might become dominant. Two of them will be discussed here:

a) The extra current might represent the contribution of latent charge carriers, e.g., hydrogen ions

b) the elevated conductance might be caused by increased ionic concentrations at the interface due to negative surface charges on the membrane.

To rule out effects like these, two types of control experiments were performed:

1) *pH-effects.* pH was measured for some of the very dilute electrolytes immediately before and after the conductance measurements. pH values ranged between 5.1 and 6. According to the conductance data obtained for pure HNO_3 solutions (Fig. 2*B* and Table 1), a channel conductance of approximately 0.06 pS is expected for an ionic activity of 10^{-5}. This is negligibly small compared to all conductance values measured. In one case, a 3 mM CsCl solution, from which conductance data had been obtained at pH 5.7, was acidified to a pH of 4.2 by adding HCl. Thereupon conductance was determined again. The two measurements did not differ significantly. Thus, the hypothesis that a major portion of the measured conductance is contributed by H^+ cannot be maintained.

2) *Possible surface charges due to contamination.* Although Glyceryl-mono-oleate is a neutral lipid, there might be a small surface charge density due to charged, surface-active impurities in either the lipid or the electrolyte. As discussed in *Methods*, there are, indeed, indications for such contaminations under certain conditions. These show up as increases in membrane conductance over a time span of 10–30 min. Under these circumstances the question must be asked, whether all the deviations from a simple binding curve, as described above, might be produced by surface charge.

An attempt was made to fit NaCl, CsCl, and $TlNO_3$ data under the assumptions of a single-site binding curve and elevated surface activities at the membrane. The latter were calculated according to the Boltzmann law, with surface potentials as derived from Gouy-Chapman theory (with the surface charge density as free parameter, *see* McLaughlin *et al.*, 1970). All the data could be fitted rather nicely assuming surface charge densities between 1 electronic charge per 8,000 $Å^2$ and 1 electronic charge per 12,000 $Å^2$.

In order to rule out this interpretation (termed "surface charge theory" in the following), some experiments were performed at constant ionic strength. Ionic strength of $TlNO_3$ solutions was maintained constant at 0.0051 by additions of $MgSO_4$ while varying the concentration of $TlNO_3$ between 0.6 and 5 mM. $MgSO_4$ itself is impermeable, and it is not expected to block other ions at this concentration (*see* Bamberg & Läuger, 1977). The low value for ionic strength of 0.0051 was selected such that the limiting laws for activity coefficient corrections and Gouy-Chapman theory would still be applicable. As indicated in Fig. 4, there is hardly a significant difference between conductance values mea-

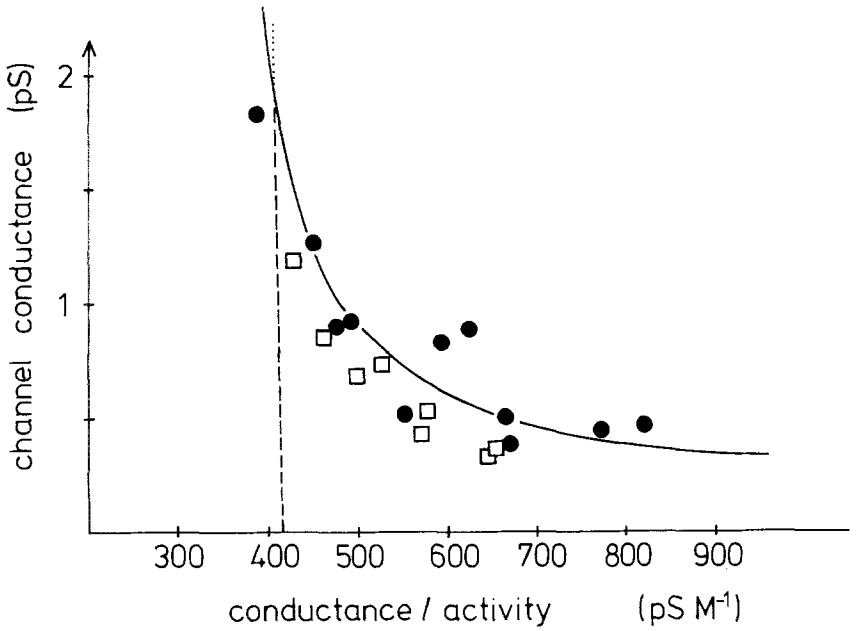

Fig. 4. Eadie-Hofstee representation of $TlNO_3$ data at low concentrations (0.6–5.1 mM). $-\bullet-$, pure $TlNO_3$; $-\square-$, $TlNO_3$ plus $MgSO_4$ to maintain ionic strength at 0.0051. The theoretical curves were calculated according to $G=G_{max}\ (1+1/Ka')^{-1}$, with $G_{max}=117$ pS, $K=2.55$, and a surface activity a' as calculated from Gouy-Chapman theory (surface charge density $\sigma=1$ electronic charge/12,000 Å). For the continuous curve, surface potential was allowed to change as the ionic strength of the $TlNO_3$-solution varied between 0.0006 and 0.0051, whereas for the broken curve, surface potential was fixed to its value for an ionic strength of 0.0051

sured with and without the $MgSO_4$ additions. The continuous and broken lines in Fig. 4 are the predictions of the "surface charge theory" for both cases. Surface charge density was chosen as 1 electronic charge/12,000 Å^2 to fit the data in the absence of $MgSO_4$. Values for limiting conductance and binding constant of the assumed single-site binding curve were $G_{max}=117$ pS and $K=2.55$ M^{-1} for a best fit in the medium concentration range. In the case of constant ionic strength the "surface charge theory" predicts a linear relationship in the Eadie-Hofstee representation: All activities are merely scaled by a constant factor, since surface potential is constant. The broken line in Fig. 4 was therefore calculated as a simple binding curve with a modified binding constant K':

$$K'=K\cdot\exp(-\psi)$$

where ψ is the Gouy-Chapman potential in units of kT/e at 5 mM ionic strength. This prediction is clearly in conflict with the data in Fig. 4. The "surface charge theory" therefore does not explain the characteristic low concentration behavior. The small differences, however, between values with and without $MgSO_4$ additions (Fig. 4) may be due to some charged impurity. It should be pointed out, however, that the data points shown in Fig. 4 are the ones most sensitive to such disturbances in this investigation.

Single Channel Conductance in Salt Mixtures

Mutual blocking among different ionic species in gramicidin A channels was described by Andersen (1975) and Neher (1975). The theory of Sandblom *et al.* (1977) accounts for these effects in terms of the present parameters from single salt conductance and parameters extracted from potential measurements in salt mixtures in the companion paper to follow. A few more examples will therefore be given here and interpreted in terms of this theory.

Fig. 5*A* illustrates "mole fraction experiments" at 10 and 100 mM total concentrations, i.e., the sum $c_{TlCl}+c_{KCl}$ is maintained constant, and conductance is plotted *vs.* % value of TlCl in the mixture. (The 100 mM data were obtained with fluoride salts for solubility reasons.) At these concentrations the terms containing mixed binding constants in the conductance expression (K^h_{xxy} and K^h_{yyx} in Eq. (52) of Sandblom *et al.*, 1977) give negligible contributions, and the curve is predicted by the theory without introducing new adjustable parameters. The solid lines in Fig. 5*A* give the predictions of the theory with parameters taken from conductance data in single salt solution (Table 2) and two parameters taken from potential measurements in salt mixtures ($\gamma_{Tl}=80\,M^{-1}$; $\beta_K=16\,M^{-1}$; *see* Eisenman *et al.*, 1978). Fig. 5*B* shows a similar experiment at 1 M total concentration (KF-TlF). In this case the choice of higher order mixed binding constants $K_{Tl,Tl,K}$ does influence the prediction of the model. Three theoretical curves are therefore given. They show that $K_{TlTlK}\simeq 0.3$ results in a reasonable fit.

In the case of 1 M salts, data and theory do not agree at low Tl^+-concentrations (left end of plot). Theory does not predict as steep a decline as is seen experimentally. These discrepancies reflect deviations in the fit of the conductance-concentration relation for thallium salts (Fig. 3*D*) at intermediate concentrations. In both cases theory predicts

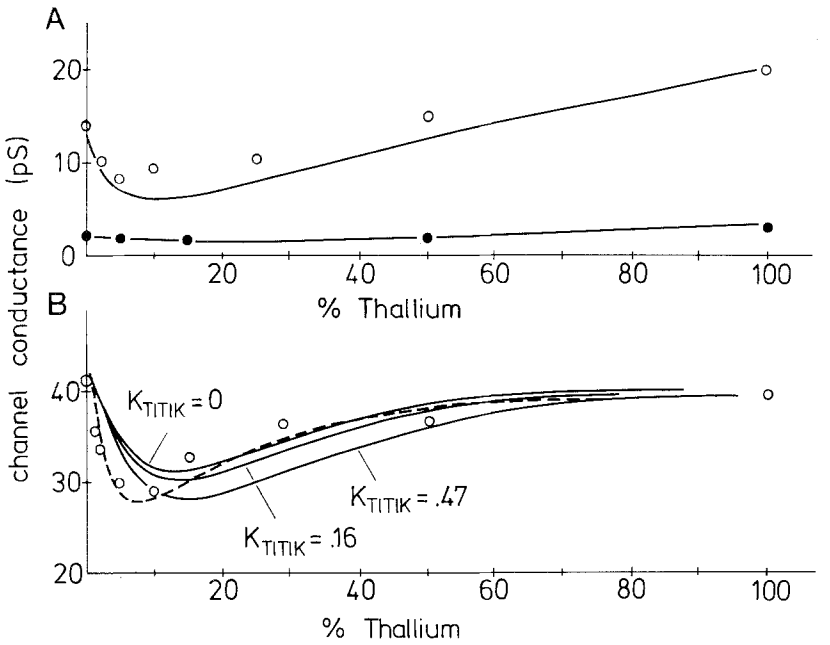

Fig. 5. Single channel conductance versus TlCl (or TlF) concentration, when a mixture of TlCl and KCl (or TlF and KF) is present symmetrically on both sides of the membrane. (*A*): The total concentration $c_{TlX}+c_{KX}$ is kept constant at 10 mM (−●−, chloride as an anion) and at 100 mM (−○−, fluoride as an anion). The continuous lines give the predictions of the theory [Sandblom *et al.*, 1977, Eq. (52)] using parameters as given in the text. (*B*): Same at 1 M total concentration (fluoride salts). Three different theoretical curves (solid) are given for three different values of the parameter K_{TlTlK}. The broken line is the best fit to the extended theory with parameters as given in the legend to Fig. 3 (*see* text)

too high conductance values, when Tl^+ is present at about 5–50 mM. As in Fig. 3*D*, the fit is considerably improved using the extended theory to allow for anion binding.

Blocking of channel conductance by *divalent* ions was recently described by Bamberg and Läuger (1977). We want to point out an important difference between the Tl^+-block reported here and the divalent ion block. Divalent ion block, as described by these authors, is accentuated by high membrane voltage. Our data show, in contrast, that the blocking phenomenon studied here is relieved by high membrane voltage: Replacing 20 mM NaAc in a 1 M NaAc solution by TlAc reduces channel amplitude by 28% at 30 mV membrane potential, by 24% at 50 mV and only by 14% at 100 mV. Thus, membrane voltage decreases the degree of block.

Discussion

Independently from a particular energy profile, any rate-theory model for ion permeation through a channel should predict a linear relationship between conductance and salt concentration in the limit of low ionic concentrations. Deviations from linearity reflect interactions among ions – for instance, competition for a binding site or electrostatic repulsion (Läuger, 1973). In this publication we present evidence that interactions between ions, passing the gramicidin channel, occur at extremely low ionic concentrations. Thus, in symmetrical solutions of TlCl, significant deviations from linearity occur in the concentration range 0.5–1 mM, where the conductance is less than 1% of the maximum conductance. Interestingly, conductance at medium concentrations (10–100 mM) is closer to linearity than at these very low concentrations. Trivial explanations for the interactions, like surface charge effects or complications by a latent charge carrier (H^+) are ruled out through control experiments at constant ionic strength and different pH-values.

Any sufficient model should allow for multiple occupancy of the channel, since both the general one-ion-model by Läuger (1973) and a specific two-compartment model by Hladky (1972) predict linear conductance-activity-relations at low concentrations. We chose to restrict our considerations to symmetrical models (basically assuming head-to-head dimerization) with a main barrier located in the center (for mathematical simplicity), and developed a theory for the simplest case within this class (Sandblom *et al.*, 1977). The model allows for four simultaneously occupyable binding sites (two in each half of the channel, i.e., on each side of the central main barrier). By exploiting the symmetry of the channel, and assuming insignificant interaction between the two outermost binding sites, the binding properties are simplified to those of a two-site model.

In the following we attempt an intuitive, qualitative explanation, in the framework of this model, of the observed variations in channel conductance when concentration of a single salt (numbers refer to Tl^+-salts) is raised symmetrically on both sides of the membrane: At the lowest concentration (below 0.5 mM) the channel is unoccupied most of the time and occupied by a single ion otherwise. No interactions between ions occur, and conductance is expected to increase linearly with concentration, since probability of ion flow across the central barrier increases with the occupancy of a first binding site. At approximately 1 mM (at about 10 mM for CsCl and at higher concentrations for other cations)

any one of the binding sites is occupied half of the time and retards the entry of additional ions, through electrostatic repulsion. This leads to a saturating behavior. Experimentally this concentration region is characterized by a high binding constant ($K^0_{Tl} \simeq 1000\,M^{-1}$) and a low limiting conductance ($G^0_{Tl} \simeq 1$ pS, *see* Eadie-Hofstee plots, Fig. 3*D*). As concentration is raised further, additional binding sites are loaded in spite of electrostatic repulsion. As was pointed out in the theoretical paper (Sandblom *et al.*, 1977), this is physically reasonable for the case of one binding site being very close to the channel mouth, particularly if one takes into account the polarizability of the ionic cloud in the aqueous medium. In the multiply loaded channel any inner ion does not obtain as deep an energy minimum at its binding site as in the singly occupied one. Thus, the medium concentration range is characterized by a lower binding constant K^h_{Tl} (steeper slope in Eadie-Hofstee representation) and a higher limiting conductance G^h_{Tl}, due to a smaller energy barrier between inner binding site and the central peak. Actually, the inner binding site to peak energy differences might be quite similar in the singly and doubly occupied states; however, the effective barrier height in the former state is the sum of the actual inner site to peak energy difference and the logarithm of the partition factor between inner and outer sites (*see* Eq. (42a) of Sandblom *et al.* 1977). For Tl^+ the values are $K^h_{Tl} \simeq 5.1\,M^{-1}$ and $G^h_{Tl} \simeq 77$ pS. The binding constant can now no longer be precisely identified with that of any particular channel state; although it corresponds approximately to that for loading the inner site when both outer sites are occupied. Exact relationships between K^h_x and equilibrium constants of individual channel states together with similar expressions for limiting conductances, etc., are given in Eqs. (42)–(44) of Sandblom *et al.* (1977).

Finally, at highest concentrations all four binding sites are occupied. In this state the channel is no longer conductive since any ion attempting to cross the central barrier has to find an empty site on the other side for a successful jump. Conductance decreases with increasing concentration. This occurs at a concentration of approximately 1 M and higher. The data for the group *1A* cations and for Tl^+ were analyzed in terms of the model of Sandblom *et al.* (1977) and the characteristic experimental parameters K^0, G^0, K^h, G^h and K^∞ were determined. They are listed in Table 2. Comparing different cations, it is obvious that differences in low and medium concentration behavior are largest for Tl^+ and pronounced for Cs^+. A distinction between the two limits is still possible for Rb^+ and K^+; however, the respective values for K^0 and K^h converge. For

Na^+ and Li^+ it is no longer possible to unambiguously distinguish between K^0 and K^h. In these cases the data are reasonably described by a single binding curve.

It should be pointed out that the exact values of the binding constants are meaningful only in the context of the activity coefficient corrections employed (*see Appendix*). There are obvious trends in the values for binding constants and limiting conductances. For instance the binding selectivity sequence of the group *Ia* cations is opposite for the outer and inner binding sites. The physical significance of this will be discussed in a companion paper after a comparison of model predictions based on these values with measurements of zero current potential in salt gradients (Eisenman *et al., to be published*).

The Tl^+-data, which show the strongest separation into high and low concentration regions, do also show systematic deviations from the predictions of the theory of Sandblom *et al.* (1977). As pointed out above, an influence of anions might be responsible for the discrepancies.

Blocking of ion flow by Tl^+-ions, which was described before (Andersen, 1975; Neher, 1975) is well predicted by the theory, using parameters from Table 2 and two further parameters obtained from independent measurements of zero current potential (Eisenman *et al., to be published*). The theoretical fit (Fig. 5) is obtained without introduction of further free parameters for the case of 10 and 100 mM total concentration.

A blocking phenomenon involving divalent ions was recently described by Bamberg and Läuger (1977). This phenomenon and the Tl^+-block, described here, differ in at least two important aspects: Tl^+ block is effective at very low Tl^+ concentrations; at high concentrations Tl^+ itself contributes to conductance. Divalent ion block was only found at high concentrations with the divalent ion reported to be impermeable. Secondly, as pointed out above, Tl^+ block is relieved by applying high voltage to the membrane, whereas divalent ion block is enhanced.

One aspect, not yet explained satisfactorily by the theory of Sandblom *et al.*, is the *I-V* relation. With a predominant central barrier, the theory predicts a hyperbolic *I-V* relationship. Experimentally, a hyperbolic relationship is observed only at very high concentrations. For low concentrations, saturating *I-V* relationships are found (Hladky & Haydon, 1972). On the other hand, the question must be asked, whether experimental *I-V* relationships can be unambiguously interpreted. Ion fluxes through the channel are large and are partly limited by access diffusion to the channel mouth (Anderson, 1977). Such an access limitation would, of course, be more severe at higher voltages

(Läuger, 1976) and low bath concentrations, such that experimental *I-V* curves would not reflect genuine channel properties.

It is possible that, together with the above considerations, a more trapezoidal shape of the central barrier would resolve this problem. Alternatively, the barriers between outer and inner sites might not be negligible, so that some kinetic effects may occur in the translocation between outer and inner sites.

This work was supported by National Science Foundation Grant GB 30835, U.S. Public Health Services Grant NS 09931 and Swedish Medical Research Council Grant 04138.

Appendix

Activity Coefficients and Surface Potentials

In the theory for the electrical properties of ion selective channels developed in paper *I* of this series, the boundary reactions were expressed in terms of external solution concentrations with no account taken of either surface potentials or activity coefficients. Any dependence of these parameters on external solution conditions will then be contained in the binding constants of the original theory. It is useful, however, to separate the various effects, and in this appendix the boundary reactions will be written explicitly in terms of activity coefficients and surface potentials.

Equilibrium at the membrane boundaries of an ion species I (for simplicity assumed to be a cation) is expressed in terms of its electrochemical potential, which is equal in the aqueous phase and the membrane phase (the latter indicated by the subscript s)

$$\overline{\mu_i} = \overline{\mu_{is}}. \tag{A.1}$$

From Eq. (A.1) we obtain

$$RT \ln \gamma_i C_i + F \psi_s = RT \ln N_{is}/K_{is} \tag{A.2}$$

where N_{is} is the fraction of time during which the ion I occupies the site S. ψ_s is the surface potential, K_{is} the binding constant of the ion to the site, and γ_i the activity coefficient in the external solution.

By defining two new quantities

$$a_i = \gamma_i^{\pm} \cdot C_i, \tag{A.3}$$

and

$$r = \sqrt{\frac{\gamma_i}{\gamma_a}} \cdot \exp \frac{F\psi_s}{RT} \tag{A.4}$$

Eq. (A.2) is rewritten as

$$K_{is}\, r\, a_i = N_{is}. \tag{A.5}$$

The binding constants determined from experiments using mean activity coefficients will therefore contain the quantity r. If $\gamma_i \approx \gamma_a$ and if $\psi_s \approx 0$, this quantity will approximate unity.

References

Andersen, O.S. 1975. Ion-Specificity of Gramicidin Channels. p. 369. International Biophysics Congress, Copenhagen

Andersen, O.S. 1977. Ion Transport across Simple Membranes. Macy Conference on Renal Function, Charleston, S.C.

Bamberg, E., Läuger, P., 1974. Temperature-dependent properties of gramicidin A channels. *Biochim. Biophys. Acta* **367**:127

Bamberg, E., Läuger, P., 1977. Blocking of the gramicidin channel by divalent cations. *J. Membrane Biol.* **35**:351

Cahalan, M., Begenisich, T., 1976. Sodium channel selectivity: Dependence on internal permeant ion concentration. *J. Gen. Physiol.* **68**:111

Eisenman, G., Sandblom, J., Neher, E. 1976. Evidence for multiple occupancy of gramicidin A channels by ions, *Biophys. J.* **16**:81*a*

Eisenman, G., Sandblom, J., Neher, E. 1977. Ionic selectivity, saturation, binding and block in the gramicidin A channel: A preliminary report. *In:* Metal-Ligand Interactions in Organic Chemistry and Biochemistry. B. Pullman and N. Goldblum, editors. Part **2**, pp. 1–36. D. Reidel, Dordrecht

Eisenman, G., Sandblom, J., Neher, E. 1978. Interactions in cation permeation through the gramicidin channel: Tl, K, Cs, Rb, Na, Li, H, and effects of anion binding. *Biophys. J.* (*in press*)

Fettiplace, R., Gordon, L.G.M., Hladky, S.B., Requena, J., Zingsheim, H.P., Haydon, D.A., 1975. Techniques in the formation and examination of "black" lipid bilayer membranes. *In:* Methods in Membrane Biology. E.D. Korn, editor. Vol. 4. Plenum, New York

Hille, B. 1975. Ionic selectivity, saturation and block in sodium channels. *J. Gen. Physiol.* **66**:535

Hladky, S.B. 1972. The Two-Site Lattice Model for the Pore. Ph. D. Dissertation, Cambridge University, England

Hladky, S.B., Haydon, D.A. 1972. Ion transfer across lipid membranes in the presence of gramicidin A. I. Studies of the unit conductance channel. *Biochim. Biophys. Acta* **274**:294

Läuger, P. 1973. Ion transport through pores: A rate-theory analysis. *Biochim. Biophys. Acta* **311**:423

Läuger, P. 1976. Diffusion-limited ion flow through pores. *Biochim. Biophys. Acta* **455**:493

McLaughlin, S.G.A., Szabo, G., Eisenman, G., Ciani, S.M. 1970. Surface charge and the conductance of phospholipid membranes. *Proc. Nat. Acad. Sci. USA* **67**:1268

Myers, V.B., Haydon, D.A. 1972. Ion transfer across lipid membranes in the presence of gramicidin A. II. The ion selectivity. *Biochim. Biophys. Acta* **274**:313

Neher, E. 1975. Ionic specificity of the gramicidin channel and the thallous ion. *Biochim. Biophys. Acta* **401**:540

Sandblom, J., Eisenman, G., Neher, E. 1977. Ionic selectivity, saturation and block in gramicidin A channels: I. Theory for the electrical properties of ion selective channels having two pairs of binding sites and multiple conductance states. *J. Membrane Biol.* **31**:383

Zeffren, E., Hall, P.L. 1973. The Study of Enzyme Mechanisms. John Wiley & Sons, New York